Geomechanics and Engineering, *Vol. 15, No. 2 (2018) 783-791*
DOI: https://doi.org/10.12989/gae.2018.15.2.783

Prediction models of the shear modulus of normal or frozen soil-rock mixtures

Zhong Zhou[1], Hao Yang[*1,2], Kai Xing[1] and Wenyuan Gao[1]

[1]School of Civil Engineering, Central South University, Changsha 410075, China
[2]Department of Architecture and Civil Engineering, City University of Hong Kong, Kowloon, Hong Kong, China

(Received April 8, 2017, Revised December 9, 2017, Accepted December 23, 2017)

Abstract. In consideration of the mesoscopic structure of soil-rock mixtures in which the rock aggregates are wrapped by soil at normal temperatures, a two-layer embedded model of single-inclusion composite material was built to calculate the shear modulus of soil-rock mixtures. At a freezing temperature, an interface ice interlayer was placed between the soil and rock interface in the mesoscopic structure of the soil-rock mixtures. Considering that, a three-layer embedded model of double-inclusion composite materials and a multi-step multiphase micromechanics model were then built to calculate the shear modulus of the frozen soil-rock mixtures. Given the effect of pore structure of soil-rock mixtures at normal temperatures, its shear modulus was also calculated by using of the three-layer embedded model. Experimental comparison showed that compared with the two-layer embedded model, the effect predicted by the three-layer embedded model of the soil-rock mixtures was better. The shear modulus of the soil-rock mixtures gradually increased with the increase in rock regardless of temperature, and the increment rate of the shear modulus increased rapidly particularly when the rock content ranged from 50% to 70%. The shear modulus of the frozen soil-rock mixtures was nearly 3.7 times higher than that of the soil-rock mixtures at a normal temperature.

Keywords: micromechanics; geo-composite material; shear modulus; the frozen soil-rock mixtures

1. Introduction

Soil-rock mixtures (Fig. 1) are extremely loose, non-uniform, geo-composite materials composed of coarse (i.e., broken rock block and gravel) and fine (i.e., sandy soil and clay) grains with a wide range of grain sizes (Cabalar 2011). These geo-composite materials are widely distributed and abundant in nature, and suitable for use as artificial engineering components because of their advantages of good resistance to compression performance, high shearing strength, and good permeability (Medley 1994, Parker 1997). Moreover, these materials are also widely used in flood control levees, roadbeds, and artificial foundations (Xu and Hu 2009, Zhou *et al*. 2017).

The macroscopic mechanical property of composite materials differs from that of other component materials, and is affected by the formation of various components that commonly play a different role in complex systems (Choi and Chung 1996, Bishop *et al*. 2006, Lee and Pyo 2008). Moreover, composite materials are composed of only two types of materials (Hashin 1964). The Parallel model (Voigt model) and series model (Reuss model) are the most representative and commonly used among all theoretical models (Wang and Pan 2008, Zhou *et al*. 2016a). Mohammadi *et al*. (2016) conducted the soil-concrete interface tests through a direct shear apparatus, and their results showed that the concrete surface texture positively affects soil-concrete interface shear strength. Azadegan *et al*. (2014) proposed an alternative method that uses the unconfined compressive strength and estimating functions available in literature to evaluate the shear strength parameters of the treated materials. However, these models can only provide the upper and lower shear modulus of the soil-rock mixtures and cannot accurately predict the effective shear modulus (Wong and Bollampally 1999). Therefore, the mechanical behaviour of composite materials in two or more phases should be analysed based on micromechanics to realise value prediction (Yang and Huang 2009, 2011).

The shear modulus of soil-rock mixtures can be used to predict the landslide mechanism of accumulation slope and to design roadbed padding made of coarse soil. Tu *et al*. (2016) investigated the parameters of shear strength and stiffness through experiments, and proposed a method of estimating the safety factor of soil slopes under wetting-drying cycles. However, research on the elastic characteristic of soil-rock mixtures is still based on engineering experience (Zhou *et al*. 2009, Zhou *et al*. 2016b). The main methods currently used to determine the shear modulus of soil-rock mixtures are test and empirical equation methods (Sitharam and Vinod 2010, Sridharan *et al*. 2006). Test methods involve an indoor or in situ test to determine the shear modulus of soil-rock mixtures. Yoshimoto *et al*. (2016) performed a series of indoor drained triaxial compression tests on a composite material and discovered that the shear strength and deformation behaviours of granulated coal ash are largely determined by the material's relative density or void ratio. However, the indoor test method is a time-consuming job and can only determine shear modulus after a soil-rock mixture has been

*Corresponding author, Postgraduate Research Assistant
E-mail: yanghaocsu@163.com

http://www.techno-press.org/?journal=gae&subpage=7 ISSN: 2005-307X (Print), 2092-6219 (Online)

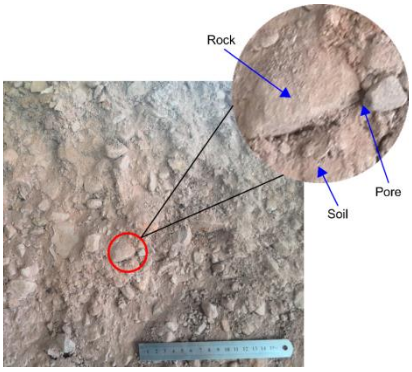

Fig. 1 Composition of a typical soil-rock mixture

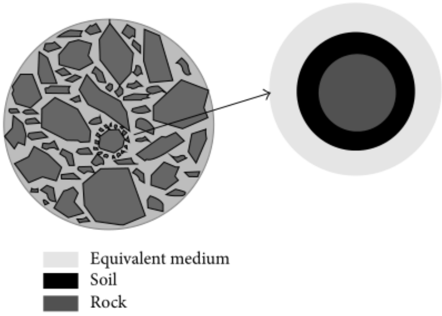

Fig. 2 Two-layer embedded model and microstructure sectional drawing of the soil-rock mixture

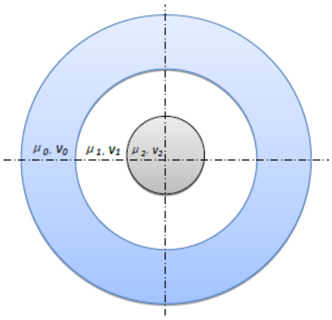

Fig. 3 Microstructure model of elastic parameter calculation

created, and the in-situ test method is costly and may not achieve the desired test accuracy because of problems with testing equipment (Zhou 2006). Moreover, the scope of various empirical equation methods is conditional. If the actual condition differs from that in the empirical equation method, then the predicted results obtained by the empirical equation method may present significant errors. In fact, both test and empirical equation methods at the macro level do not reflect the mechanical properties at microscopic scales (Ghazavi 2004, Sitharam and Nimbkar 2000). Therefore, an appropriate micromechanical model must be established to accurately predict the shear modulus of soil-rock mixtures in the design stage to achieve effective design applications in slope retaining and roadbed padding engineering (Yang 2007, Huang and Yang 2014).

Furthermore, soil-rock mixtures are widely distributed in frozen ground areas throughout the world (Kim and Park 2017). Freeze-thaw cycles damage cause these mixtures. Similarly, Chen *et al*. (2016) discovered that cyclic loading causes damage to rock salt, and confining pressure exerts a significant effect on the unloading modulus due to the variation in mechanical parameters. With the development of engineering construction in cold regions, research on the freeze-thaw action in soil-rock mixtures has shifted from an overall study to the elaboration of the effect of various physical and mechanical parameters through tests and theoretical analyses (Xiao and Chen 2001, Yang *et al*. 2014, Kim *et al*. 2017). However, research on shear modulus of frozen soil-rock mixtures is only in the preliminary exploration stage because the microstructure of soil-rock mixtures at freezing temperatures is more complicated than that at normal temperatures (Yang *et al*. 2015). Therefore, building a theoretical model of the shear modulus of frozen soil-rock mixtures from the micromechanics perspective is necessary and applicable.

In this study, considering rock particles wrapped by soil matrix embedded in the equivalent medium composite materials (Fig. 2), the single-inclusion model of two-layer embedded composite materials was applied to predict the shear modulus of a soil-rock mixture at a normal temperature. Considering ice-rock particles wrapped by frozen soil matrix embedded in the equivalent medium composite materials, the double inclusion model of three-layer embedded composite material was applied to predict the shear modulus of the soil-rock mixtures at a freezing temperature, and the ice-rock particles were regarded as a two-layer embedded composite material that consisted of rock particles wrapped by the ice matrix and was embedded in the equivalent medium composite material (Fig. 6).

2. Model of the shear modulus of a normal soil-rock mixture

As for soil-rock mixtures at a normal temperature, in consideration of rocks wrapped by soil in the mesoscopic structure, a two-layer embedded model of single-inclusion composite material was built to calculate its shear modulus.

2.1 Single-inclusion model of shear modulus

First, in view of the inclusion of the composite, a two-layer embedded model was built. The inclusion of each particle was regarded as circular. Each particle was wrapped by a substrate of a certain thickness, and embedded in an infinite equivalent composite medium, as shown in Fig. 2.

The rocks in the soil-rock mixture were composed of pebbles with a spheroid shape or broken rocks with a cuboid shape. The rocks were distributed randomly, and inlaid in the 3D structure of the soil-rock mixtures. Therefore, the 2D structure of cross sections of the soil-rock mixture was not unique. In this situation, the cylindrical-fiber micromechanics model can provide a more suitable description of the 2D section of the soil-rock mixtures.

Assuming that the inclusion phase is homogeneous and isotropic, on the basis of the theoretical equation of single-inclusion composite shear modulus derived by Christensen and Lo (1979) and with the two-layer embedded model shown in Fig. 3, the effective shear modulus μ_0 is calculated as following equations.

$$[\mu_0/\mu_1]^2 A + [\mu_0/\mu_1] B + D = 0 \quad (1)$$

$$A = 3f(1-f)^2(\mu_2/\mu_1-1)(\mu_2/\mu_1+\eta_2)+ \left[(\mu_2/\mu_1)\eta_1+\eta_2\eta_1-((\mu_2/\mu_1)\eta_1-\eta_2)f^3\right]\times \left[f\eta_1(\mu_2/\mu_1-1)-((\mu_2/\mu_1)\eta_1+1)\right] \tag{2}$$

$$B = -6f(1-f)^2(\mu_2/\mu_1-1)(\mu_2/\mu_1+\eta_2)+ \left[(\mu_2/\mu_1)\eta_1+(\mu_2/\mu_1-1)f+1\right]\times \left[(\mu_2/\mu_1+\eta_2)(\eta_1-1)-2((\mu_2/\mu_1)\eta_1-\eta_2)f^3\right]+ (\eta_1+1)f(\mu_2/\mu_1-1)\left[\mu_2/\mu_1+\eta_2+((\mu_2/\mu_1)\eta_1-\eta_2)f^3\right] \tag{3}$$

$$D = 3f(1-f)^2(\mu_2/\mu_1-1)(\mu_2/\mu_1+\eta_2)+ \left[(\mu_2/\mu_1)\eta_1+(\mu_2/\mu_1-1)f+1\right]\times \left[\mu_2/\mu_1+\eta_2+((\mu_2/\mu_1)\eta_1-\eta_2)f^3\right] \tag{4}$$

$$\eta_1 = 3-4\nu_1, \eta_2 = 3-4\nu_2 \tag{5}$$

where μ_0, μ_1, and μ_2 are the shear modulus of the soil-rock mixtures, the soil, and rock, respectively. After integrating Eqs. (2)-(5) into Eq. (1), the shear modulus of the soil-rock mixtures can be calculated, based on the relationship between the elastic constants.

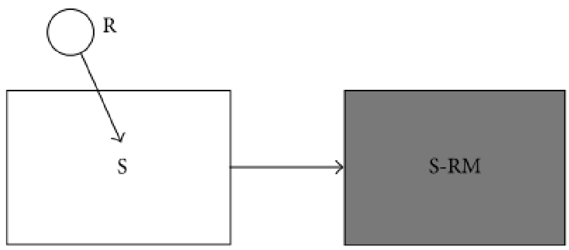

Fig. 4 Schematic of the calculation of the single inclusion problem

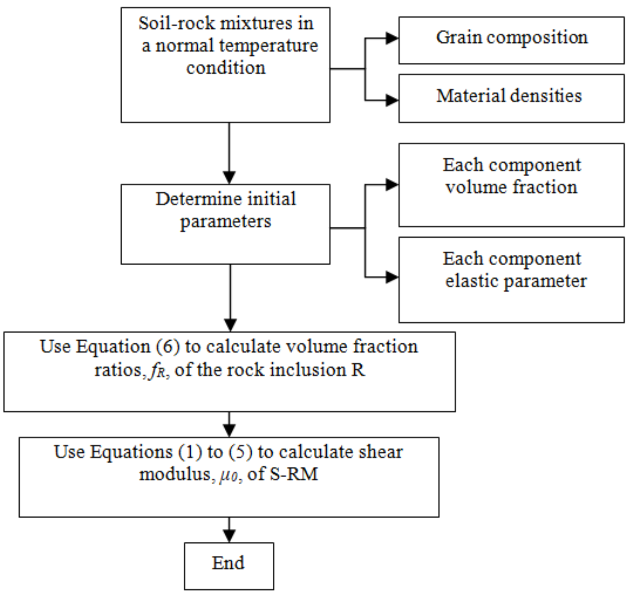

Fig. 5 Flowchart of the calculation of the shear modulus of the soil-rock mixture

2.2 Schematic calculation of the single-inclusion model

A soil-rock mixture at a normal temperature can be seen as a single inclusion composite material. The main calculation process involves integrating the rock inclusion into the soil matrix material first, and then using Eq. (6) to complete the homogenization process, thereby obtaining the macroscopic properties of the soil-rock mixtures at a normal temperature. Elastic characteristic of rock inclusion is denoted as R, and determined by certain material properties such as shear modulus μ and Poisson's ratio v, etc. Elastic characteristic of the soil matrix is denoted as S, and the elastic characteristic of the soil-rock mixture is denoted as S-RM. The process is detailed in detail in Fig. 4.

After that rock inclusion R is eliminated, the volume fraction ratio of rock inclusion R can be derived as follows

$$f_R = \frac{V_R}{V_S+V_R} \tag{6}$$

where V_S is the volume of the soil, and V_R is the volume of the rock.

2.3 Calculation process of the single-inclusion model

The flowchart in Fig. 5 illustrates the calculation process of the shear modulus of the soil-rock mixture at a normal temperature on the basis of the preciously presented micromechanics analysis and in consideration of the characteristics of the composite materials of the soil-rock mixture at a normal temperature.

3. Shear modulus model of a frozen soil-rock mixture

The pores in a soil-rock mixture are of three types: innate pore in the soil, which is called soil pore; the inherent pore in the rock grain pore, which is called rock pore; and the pore between the soil and rock grain, which is called structural pore. The structural porosity can be determined based on the inherent porosity of the soil-rock mixture, soil, and rock grain. This study assumed that the soil and rock grain are two entirely independent research objects. Thus, the calculation model must regard pore structure as the inclusion for the soil-rock mixtures.

Rocks cannot be completely wrapped by soil because of the pore structure in the contact interface between the soil and rock grain of soil-rock mixtures. This scenario reveals the loose property of soil. The water in the pore structure freezes with a reduction in temperature. The existence of the pore structure and the adsorption on the surface of the rock indicate that the contact surface also exists in the ice interface between the rock grain and soil. A three-layer embedded model of a double-inclusion composite material and a multi-step multiphase micromechanics model were built to calculate the shear modulus of the frozen soil-rock mixtures, in consideration of the ice interface interlayer attached between soil and rock grains in the mesoscopic structure of the soil-rock mixture at a freezing temperature.

In previous Section 2, the influence of pore structure in

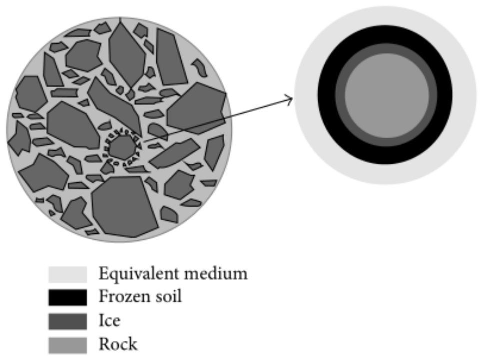

Fig. 6 Three-layer embedded model and microstructure sectional drawing of the frozen soil-rock mixture

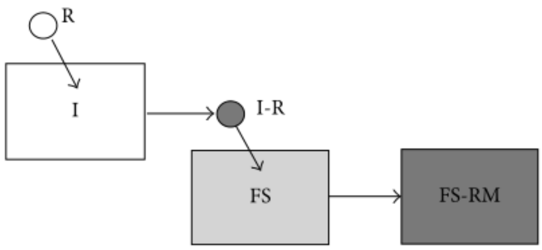

Fig. 7 Schematic diagram of the stepping scheme for the multiphase double inclusion problem

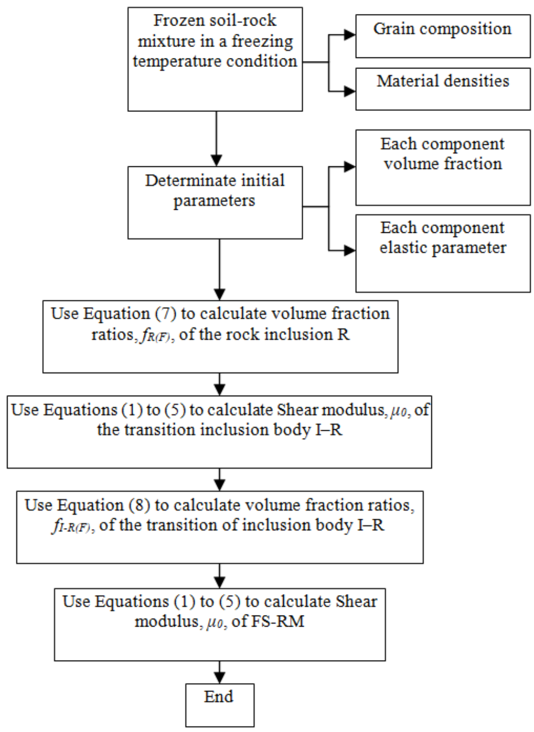

Fig. 8 Flowchart of the calculation of the shear modulus of the frozen soil-rock mixture

the contact interface on the shear modulus of the soil-rock mixture was not considered. And the three-layer embedded model of a double inclusion composite material in Section 3 can be used to recalculate the shear modulus of the soil-rock mixtures at a normal temperature to evaluate the predicted effect by comparing the two model calculations with the test data.

3.1 Double-inclusion model of shear modulus

First, the three-layer embedded model was built based on the case of the double-inclusion composite. The inclusion of each particle was regarded as circular inclusion wrapped by a substrate with a certain thickness and embedded in an infinite equivalent composite medium. The model is shown in Fig. 6.

A mechanical method the divides the whole into parts and a gradual solution were used to simplify the three-layer embedded model. The rock at the core and the wrapped outer interface were extracted and regarded as the research model or single mixed micromechanical model. Its equivalent shear modulus was calculated by using the two-layer embedded model of the single-inclusion composite material, and was called the transition inclusion body. Next, the three-layer embedded model was considered an entire research object. The rock at the core and the wrapped outer ice interface were converted into a transition inclusion body through a step-by-step process. Thus, the entire model was seen as a two-layer embedded model composed of a transition inclusion body with a frozen soil substrate. Its equivalent shear modulus parameters (elastic parameters of the soil-rock mixtures at freezing condition) were calculated.

3.2 Schematic calculation of the double-inclusion model

The frozen soil-rock mixture can be seen as a multiphase double-inclusion composite material. Thus, the multi-step model was utilised to handle each inclusion and the shear modulus of the composite material was calculated step-by-step (Yang and Tao 2007).

In this above step-by-step process, firstly, the rock inclusion (assuming that the elastic characteristic is R) was integrated into the ice interface matrix material (assuming that the elastic characteristic is I), and Eqs. (1)-(5) were used to complete the homogenisation process and calculate the transition inclusion body (assuming that the elastic characteristic is I-R). Secondly, after homogenisation, the composite material I-R was used as a new inclusion, and the new inclusion I-R was integrated into the frozen soil matrix (assuming that the elastic characteristic is FS). Thirdly, Eqs. (1) to (5) were adopted to complete the homogenisation process. Finally, the macroscopic properties (assuming that its elastic characteristic is FS-RM) of the soil-rock mixtures at a freezing condition were calculated. The entire calculation process is shown in detail in Fig. 7.

When rock inclusion R was eliminated, the volume fraction ratio of rock inclusion R was derived as follows

$$f_{R(F)} = \frac{V_R}{V_I + V_R} \tag{7}$$

When the transition of inclusion body I-R was included, the volume fraction of inclusion body I-R was derived as follows

$$f_{I-R(F)} = \frac{V_I + V_R}{V_{FS} + V_I + V_R} \quad (8)$$

where V_I is the volume of the ice interface, V_R is the volume of the rock, and V_{FS} is the volume of the frozen soil.

3.3 Calculation process of the double-inclusion model

The flowchart shown in Fig. 8 illustrates the calculation process of the shear modulus of the frozen soil-rock mixture on the basis of the preciously presented micromechanics analysis, and in consideration of the characteristics of the materials of the frozen soil-rock mixture.

4. Comparison of models and tests

The elastic properties and density fraction ratio of soil and rock grains in the soil-rock mixtures must be determined before calculating the shear modulus of the soil-rock mixture by using the method proposed in this paper. Measuring critical parameters (i.e., rock content ratio, porosity of soil-rock mixture and density of different types of aggregates) makes sure that the density fraction ratio of each phase of the soil-rock mixtures can be calculated. The shear modulus of soil-rock mixtures can be simply calculated according to a method previously provided. The calculation process is illustrated in Figs. 5 and 8.

Guo (1998) reported that 5 mm is the soil-rock boundary particle size widely used in engineering, and recommended it as the boundary of sand and gravel in research on classification and naming of soil-rock mixtures. Using this boundary, the present study utilised all fine aggregates with a particle size of less than 5 mm as the soil substrate. In the calculation process, the coarse aggregates which were regarded as the inclusion were placed individually. The volumetric percentage of coarse grains is called rock content, and denoted as C_R.

4.1 Volume fractions

With the above two models, the shear modulus of the soil-rock mixtures was calculated with different rock contents at 20 ℃ (referred to as S-RM) and -20 ℃ (referred to as FS-RM). The test samples were prepared, and their modulus of elasticity was tested indoors. Moreover, the water content of every sample was saturated. Through the experiments, the relationship was comprehensively analysed, and the difference between the values of the model and test was calculated. When the rock contents were similar, S-RM and FS-RM were actually the same rock gradation samples.

The volume fractions of the composite material were easily calculated in each phase according to the data on the rock content, measured porosity, and density of each composed material of the soil-rock mixture. S-RM with five different rock contents and its volume fractions are listed in Table 1. For the saturated soil-rock mixture with similar gradation, the volume fraction ratio of ice interface of FS-RM is equal to that of the pore structure of S-RM.

4.2 Shear modulus obtained by the proposed models

Table 1 Volume fraction of S-RM with different rock contents

Rock content (%)	Volume fraction of S-RM (%)		
	Soil	Rock	Structural pore
30	69.21	30.00	0.79
40	58.98	40.00	1.02
50	48.75	50.00	1.25
60	38.68	60.00	1.32
70	28.14	70.00	1.86

Table 2 Shear modulus of soil and frozen soil

Medium	Testing temperature (℃)	Shear modulus (MPa)
Soil of S-RM	20	0.94
Frozen soil of FS-RM	-20	3.68

Table 3 Shear modulus model calculation values of S-RM and FS-RM

Rock content (%)	Shear modulus model calculation values (MPa)		
	S-RM (2–layer)	S-RM (3–layer)	FS-RM (3–layer)
30	1.714	1.758	6.715
40	2.248	2.295	8.669
50	3.092	3.125	11.660
60	4.475	4.438	16.392
70	7.056	6.697	25.228

Soil samples with a diameter of 100 mm and a height of 200 mm were fabricated (the water content of the sample was saturated). The elastic parameters of soil and frozen soil were measured at 20 and -20℃, respectively. The test results are shown in Table 2.

Rock samples with a diameter of 25 mm and a height of 50 mm were also fabricated. The elastic parameters were tested by using the strain gauge method. The measured data in this paper were combined with the research findings of Wang *et al*. (2008). The shear modulus and Poisson's ratio of the rock, soil, frozen soil and ice interface were 16,667 MPa and 0.2, 0.94 MPa and 0.4, 3.68 MPa and 0.38, and 2,623 MPa and 0.3 respectively.

The pore structure was formed because of the incomplete parcel of soil and rock. Thus, structure pore and soil coexisted on the contact surface of the rock grain. The equivalent elastic property of the rock package should range between those of soil and pore structure water. Considering that, this paper regarded the equivalent elastic property as 0.5 times that of the soil elastic property. After this step, the two-layer embedded model of single-inclusion composite materials was used to calculate the shear modulus of S-RM. And the three-layer embedded model of double-inclusion composite materials was also used to calculate the shear modulus of S-RM and FS-RM. The calculation results are shown in Table 3.

Table 3 shows that the shear modulus of the soil-rock mixtures at a freezing temperature is significantly higher than that at normal temperature. Furthermore, with the increase in rock content, the shear modulus gradually increased regardless of temperature. This phenomenon is consistent with engineering experience.

(a) TAJ-2000 large static triaxial test apparatus

(b) Permafrost natural environment simulation system

Fig. 9 Equipment used in this study

(a) Compacted specimen

(b) Prepared chamber for confining pressure

Fig. 10 The compacted specimen and prepared chamber

Table 4 Shear modulus values of S-RM and FS-RM

Rock content (%)	Shear modulus values by test (MPa)	
	S-RM (test)	FS-RM (test)
30	1.785	6.866
40	2.344	8.449
50	3.219	11.306
60	4.194	15.734
70	6.276	23.271

4.3 Shear modulus obtained by laboratory test

To verify the results of the shear modulus of S-RM and FS-RM calculated by the above two models, this paper measured the shear modulus of S-RM and FS-RM with five different rock contents by using the following test method.

The samples were prepared as follows. Firstly, soil samples obtained from the field were dried and sieved, and they were divided into two parts, i.e., soil with a range of 0 mm to 5 mm and gravel with a range of 5 mm to 60 mm. Secondly, considering the requirements of volume percentage C_R of gravel, the different samples were prepared with saturated water content. In the experiment, the diameter and height of the samples were 300 and 600 mm, respectively, and the samples were fabricated in strict accordance with geotechnical experimental procedures. The distribution of the sample particles should be uniform. The compaction process was divided into five layers, and compaction control was set to 95% to ensure a uniform distribution. For the rock content, the soil and rock samples were mixed completely. A typical soil-rock mixture was used to measure its natural moisture content. The quality of each layer of the soil-rock mixtures was calculated based on the maximum dry density of soul samples in the compaction test. The completely mixed soil-rock mixture was placed in a compaction cylinder five times for manual compaction. The quality of each layer was controlled to one-fifth of the total mass. The compaction of the layer was continuous until the height of each soil layer reached 12 mm, which is one-fifth of the total cylinder height after compaction process. The surface of each layer was roughened before adding the soil layer to the next layer to ensure that no weakness plane appears after compaction, which can contribute to improved combination between layers and can enhance sample integrity. The mould barrels were immediately removed when the compaction of all five layers was completed.

In the test, a TAJ-2000 large static triaxial test apparatus (Fig. 9(a)) and a permafrost natural environment simulation system (Fig. 9(b)) in the *National Engineering Laboratory* of *High-speed Railway Construction Technology* of Central South University were used as test equipment. The maximum axial stress of the triaxial test apparatus was 2000kN, and the maximum confining pressure was 10MPa. In this study, as shown in Fig. 10(a), the sample diameter was 300 mm, and height was 600 mm, and the maximum particle diameter was 60 mm. The confining pressure cylinder was pushed in place below the loading oil rod axis of the triaxial test apparatus, as shown in Fig. 10(b).

According to the above test method, the shear modulus of the soil-rock mixture with different rock contents was in the same compaction condition. The experiment results are shown in Table 4.

Table 4 shows that the shear modulus of the soil-rock mixture under the freezing temperature condition was significantly higher than that under the normal temperature condition. With the increase in the rate of rock content, the shear modulus of the soil-rock mixture gradually increased under freezing and normal temperature conditions. These above findings are consistent with the results obtained by the micromechanics calculation model, which proves that the calculation model proposed in this study is effective and meaningful.

Table 5 Relative error chart between model calculation values and the measured test values

Rock content (%)	Relative error (%)		
	S-RM (2–layer)	S-RM (3–layer)	FS-RM (3–layer)
30	-4.0	-1.5	-2.2
40	-4.1	-2.1	2.6
50	-3.9	-2.9	3.1
60	6.7	5.8	4.2
70	12.4	6.7	8.4

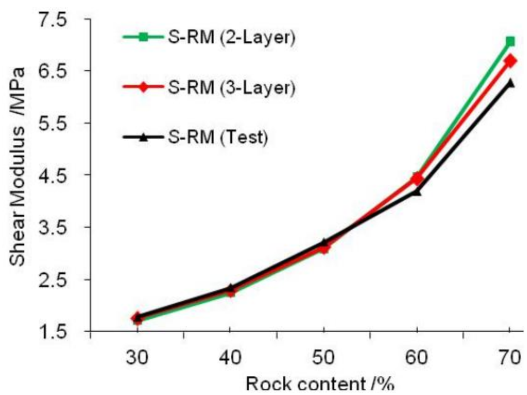

Fig. 11 Comparison between the values calculated by the soil-rock mixture model and experimental values at normal temperature condition

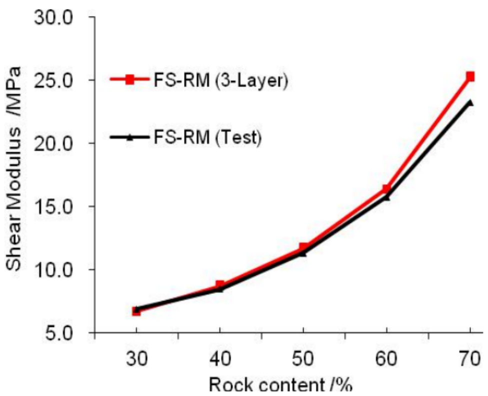

Fig. 12 Comparison between values calculated by the soil-rock mixture model and experimental values at freezing temperature condition

4.4 Comparative analysis

The calculated relative errors are shown in Table 5. These errors were obtained through a comparison of the values obtained by the proposed models (Section 4.3) and the values obtained by the experimental tests (Section 4.4). A comparison of model calculation and measured test values at a normal temperature is shown in Fig. 11, and the same comparison but at a freezing temperature is shown in Fig. 12.

Table 5 shows that the shear modulus calculated by the micromechanics model of the soil-rock mixture was basically in accordance with the experimental values. The maximum relative error did not exceed 12.4%. The predicted results of the two-layer single-inclusion model are good. However, the three-layer double-inclusion model is much better than the two-layer single-inclusion model in predicting the effect of the soil-rock mixtures at a normal temperature.

Figs. 11 and 12 show that, the shear modulus of the soil-rock mixture at a freezing temperature was significantly greater than that at a normal temperature. Comparison of the shear modulus results calculated by the model at -20 ℃ with those at 20 ℃ indicated that the average shear modulus of FS-RM was 3.76 times that of S-RM. Comparison of the shear modulus results measured at -20 ℃ with those measured at 20 ℃ showed that the average shear modulus of FS-RM was 3.68 times that of S-RM.

Regardless of temperature, with the increase in rock content, the shear modulus of the soil-rock mixture increased step by step. Moreover, the shear modulus of the soil-rock mixture increased significantly particularly when the rock content was between 50% and 70%.

The error between the values calculated by the model and the measured values can be attributed to the following reasons: first, the assumed rock shape, size, and its distribution form in the model; then, the differences in the internal structure characteristics of the soil-rock mixtures, and finally, differences in the material properties of the substrate, the composite materials, and the actual component material, among others. Although error existed between the values obtained by the model and test, the relative error was within an acceptable range, indicating that the micromechanics model proposed in this paper is reasonable and reliable.

5. Conclusions

This paper described the theoretical models for predicting the shear modulus of soil-rock mixtures at normal or freezing temperatures by using a two-layer embedded micromechanical model of single-inclusion composite materials and a three-layer embedded micromechanical model of double-inclusion composite materials. The preceding analysis led to the following conclusions.

(1) A two-layer embedded micromechanical model of single-inclusion composite materials with effective macro performance was presented in this paper. The shear modulus of the soil-rock mixtures at a normal temperature

was predicted using the model. The test results showed that the results predicted by the two-layer single-inclusion model were acceptable. However, the three-layer double-inclusion model performed better than the two-layer single-inclusion model in predicting the shear modulus of the soil-rock mixtures at a normal temperature. According to the multi-step homogenisation method, a three-layer embedded micromechanical model of double-inclusion composite materials with effective macro performance was also presented. The shear modulus of the soil-rock mixture at a freezing temperature condition was predicted using the model.

(2) In this paper, two micromechanical models were used to calculate the shear modulus of S-RM and FS-RM with rock contents of 30%, 40%, 50%, 60%, and 70% . The calculated results were compared with the test results. The maximum relative error between the results obtained by the two methods was 12.4%, which is within the acceptable range and illustrates that the two micromechanical models presented in this paper can be utilised to estimate the mechanical properties of soil-rock mixtures at normal and freezing temperatures.

(3) At normal or freezing temperatures, with the increase in rock content, the shear modulus of the soil-rock mixture increased gradually. Moreover, the shear modulus of the soil-rock mixtures increased significantly particularly when the rock content was between 50% and 70%.

(4) The shear modulus of the frozen soil-rock mixture was nearly 3.7 times higher than that of the soil-rock mixture under normal temperature condition.

Acknowledgements

The research described in this paper was financially supported by the project grant No. 50908234 funded by the National Natural Science Foundation of China, the project grant No. 2011CB710604 funded by the Major State Basic Research Development Program of China, the project grant No. 2014zzts236 funded by the Fundamental Research Funds for the Central Universities of Central South University, and the open-research grant No. SLDRCE15-04 funded by the State Key Laboratory of Civil Engineering Disaster Prevention of Tongji University.

References

Azadegan, O., Li, J. and Jafari, S.H. (2014), "Estimation of shear strength parameters of lime-cement stabilized granular soils from unconfined compressive tests", *Geomech. Eng.*, **7**(3), 247-261.

Bishop, C.M., Tang, M., Cannon, R.M. and Carter, W.C. (2006), "Continuum modeling and representations of interfaces and their transitions in materials", *Mater. Sci. Eng. A*, **422**(1-2), 102-114.

Cabalar, A.F. (2011), "The effects of fines on the behaviour of a sand mixture", *Geotech. Geol. Eng.*, **29**(1), 91-100.

Chen, J., Du, C., Jiang, D., Fan, J. and He, Y. (2016), "The mechanical properties of rock salt under cyclic loading-unloading experiments", *Geomech. Eng.*, **10**(3), 325-334.

Choi, C.K. and Chung, G.T. (1996), "A gap element for three-dimensional elasto-plastic contact problems", *Comput. Struct.*, **61**(6), 1155-1167.

Christensen, R.M. and Lo, K.H. (1979), "Solutions for effective shear properties in three phase sphere and cylinder models", *J. Mech. Phys. Solid.* **27**(4), 315-330.

Ghazavi, M. (2004), "Shear strength characteristics of sand-mixed with granular rubber", *Geotech. Geol. Eng.*, **22**(3), 401-416.

Guo, Q.G. (1998), *Engineering Properties of coarse grained soil and its Application*, Yellow River Conservancy Press, Zhengzhou, China (in Chinese).

Hashin, Z. (1964), "Theory of mechanical behavior of heterogeneous media", *Appl. Mech. Rev.*, **17**(1), 1-9.

Huang, F. and Yang, X.L. (2011), "Upper bound limit analysis of collapse shape for circular tunnel subjected to pore pressure based on the Hoek-Brown failure criterion", *Tunn. Undergr. Sp. Technol.*, **26**(5), 614-618.

Kim, D. and Park, K. (2017), "Evaluation of the grouting in the sandy ground using bio injection material", *Geomech. Eng.*, **12**(5), 739-752.

Kim, Y.M., Kwon, T.H. and Kim, S. (2017), "Measuring elastic modulus of bacterial biofilms in a liquid phase using atomic force microscopy", *Geomech. Eng.*, **12**(5), 863-870.

Lee, H.K. and Pyo, S.H. (2008), "Multi-level modeling of effective elastic behavior and progressive weakened interface in particulate composite", *Compos. Sci. Technol.*, **68**(2), 387-397.

Medley, E. (1994), "The engineering characterization of mélanges and similar block-in-matrix rocks (bimrocks)", Ph.D. Dissertation, University of California, Berkeley, California, U.S.A.

Mohammadi, A.H., Ebadi, T., Ahmadi, M. and Aliasghar, A. (2016), "Shear strength behavior of crude oil contaminated sand-concrete interface", *Civ. Eng. J.*, **2**(8), 365-374.

Parker, S.P (1997), *Dictionary of Geology and Mineralogy*, McGraw-Hill Companies, New York, U.S.A.

Sitharam, T.G. and Nimbkar, M.S. (2000), "Micromechanical modelling of granular materials: Effect of particle size and gradation", *Geotech. Geol. Eng.*, **18**(2), 91-117.

Sitharam, T.G. and Vinod, J.S. (2010), "Evaluation of shear modulus and damping ratio of granular materials using discrete element approach", *Geotech. Geol. Eng.*, **28**(5), 591-601.

Sridaran, A., Soosan, T.G., Jose, B.T. and Abraham, B.M. (2006), "Shear strength studies on soil-quarry dust mixtures", *Geotech. Geol. Eng.*, **24**(5), 1163-1179.

Tu, Y.L., Zhong, Z.L., Luo, W.K., Liu, X.R. and Wang, S. (2016), "A modified shear strength reduction finite element method for soil slope under wetting-drying cycles", *Geomech. Eng.*, **11**(6), 739-756.

Wang, M. and Pan, N. (2008), "Predictions of effective physical properties of complex multiphase materials", *Mater. Sci. Eng. R-Rep.*, **63**(1), 1-30.

Wang, Z.Z., Mu, S.Y., Niu, Y.H., Chen, L.J., Liu, J. and Liu, X.D. (2008), "Predictions of elastic constants and strength of transverse isotropic frozen soil", *Rock Soil Mech.*, **29**(S1), 475-480. (in Chinese)

Wong, C.P. and Bollampally, R.S. (1999), "Thermal conductivity, elastic modulus, and coefficient of thermal expansion of polymer composite filled with ceramic particles for electronic packaging", *J. Appl. Polym. Sci.*, **74**(14), 3396-3403.

Xiao, Z.M. and Chen, B.J. (2001), "On the interaction between an edge dislocation and a coated inclusion", *J. Solid. Struct.*, **38**(15), 2533-2548.

Xu, W.J. and Hu, R.L. (2009), "Conception, classification and significations of soil-rock mixture", *J. Hydrogeol. Eng. Geol.*, **36**(4), 50-56,70 (in Chinese).

Yang, H., Zhou, Z., Wang, X. and Zhang, Q. (2015), "Elastic modulus calculation model of a soil-rock mixture at normal or freezing temperature based on micromechanics approach", *Adv.*

Mater. Sci. Eng., 1-10.
Yang, Q.S. and Tao, X. (2007), "Stepping scheme for multi-inclusion problem", *Acta Materiae Compositae Sinica*, **24**(6), 128-134 (in Chinese).
Yang, X.L. (2007), "Upper bound limit analysis of active earth pressure with different fracture surface and nonlinear yield criterion", *Theor. Appl. Fract. Mech.*, **47**(1), 46-56.
Yang, X.L. and Huang, F. (2009), "Influences of material dilatancy and pore water pressure on stability factor of shallow tunnels", *Trans. Nonferr. Met. Soc. Chin.*, **19**(S3), 819-823.
Yang, X.L. and Huang, F. (2011), "Collapse mechanism of shallow tunnel based on nonlinear Hoek-Brown failure criterion", *Tunn. Undergr. Sp. Technol.*, **26**(6), 686-691.
Yang, Y., Gao, F., Cheng, H., Lai, Y. and Zhang, X. (2014), "Researches on the constitutive models of artificial frozen silt in underground engineering", *Adv. Mater. Sci. Eng.*, 1-8.
Yoshimoto, N., Wu, Y., Hyodo, M. and Nakata, Y. (2016), "Effect of relative density on the shear behavior of granulated coal ash", *Geomech. Eng.*, **10**(2), 207-224.
Zhou, Z., Wang, H.G., Fu, H.L. and Liu, B.C. (2009), "Influences of rainfall infiltration on stability of accumulation slope by in-situ monitoring test", *J. Central South Univ. Technol.*, **16**(2), 297-302.
Zhou, Z. (2006), "Study on the fluid-solid coupling characteristic of soil and rock blending landslide and its prediction and forecast", Ph.D. Dissertation, Central South University, Changsha, China (in Chinese).
Zhou, Z., Yang, H., Wan, Z.H. and Liu, B.C. (2016a), "Computational model for electrical resistivity of soil-rock mixtures", *J. Mater. Civ. Eng.*, **28**(8), 06016009.
Zhou, Z., Yang, H., Wang, X.C. and Zhang, Q.F. (2016b), "Fractured rock mass hydraulic fracturing under hydrodynamic and hydrostatic pressure joint action", *J. Central South Univ. Technol.*, **23**(10), 2695-2704.
Zhou, Z., Yang, H., Wang, X. and Liu, B. (2017), "Model development and experimental verification for permeability coefficient of soil-rock mixture", *J. Geomech.*, **17**(4), 04016106.

CC